Probabilistic Projections of 21st Century Climate Change over Northern Eurasia

Erwan Monier, Andrei Sokolov, Adam Schlosser,
Jeffery Scott and Xiang Gao

MIT JOINT PROGRAM
SCIENCE POLICY
GLOBAL CHANGE

MIT JOINT PROGRAM ON THE SCIENCE AND POLICY of GLOBAL CHANGE

Report No. 246
July 2013

The MIT Joint Program on the Science and Policy of Global Change is an organization for research, independent policy analysis, and public education in global environmental change. It seeks to provide leadership in understanding scientific, economic, and ecological aspects of this difficult issue, and combining them into policy assessments that serve the needs of ongoing national and international discussions. To this end, the Program brings together an interdisciplinary group from two established research centers at MIT: the Center for Global Change Science (CGCS) and the Center for Energy and Environmental Policy Research (CEEPR). These two centers bridge many key areas of the needed intellectual work, and additional essential areas are covered by other MIT departments, by collaboration with the Ecosystems Center of the Marine Biology Laboratory (MBL) at Woods Hole, and by short- and long-term visitors to the Program. The Program involves sponsorship and active participation by industry, government, and non-profit organizations.

To inform processes of policy development and implementation, climate change research needs to focus on improving the prediction of those variables that are most relevant to economic, social, and environmental effects. In turn, the greenhouse gas and atmospheric aerosol assumptions underlying climate analysis need to be related to the economic, technological, and political forces that drive emissions, and to the results of international agreements and mitigation. Further, assessments of possible societal and ecosystem impacts, and analysis of mitigation strategies, need to be based on realistic evaluation of the uncertainties of climate science.

This report is one of a series intended to communicate research results and improve public understanding of climate issues, thereby contributing to informed debate about the climate issue, the uncertainties, and the economic and social implications of policy alternatives. Titles in the Report Series to date are listed on the inside back cover.

Ronald G. Prinn and John M. Reilly
Program Co-Directors

For more information, please contact the Joint Program Office

Postal Address: Joint Program on the Science and Policy of Global Change
77 Massachusetts Avenue
MIT E19-411
Cambridge MA 02139-4307 (USA)

Location: 400 Main Street, Cambridge
Building E19, Room 411
Massachusetts Institute of Technology

Access: Phone: +1.617. 253.7492
Fax: +1.617.253.9845
E-mail: globalchange@mit.edu
Web site: http://globalchange.mit.edu/

Printed on recycled paper

Probabilistic Projections of 21st Century Climate Change over Northern Eurasia

Erwan Monier[*†], Andrei Sokolov[*], Adam Schlosser[*], Jeffery Scott[*] and Xiang Gao[*]

Abstract

We present probabilistic projections of 21st century climate change over Northern Eurasia using the Massachusetts Institute of Technology (MIT) Integrated Global System Model (IGSM), an integrated assessment model that couples an earth system model of intermediate complexity with a two-dimensional zonal-mean atmosphere, to a human activity model. Regional climate change is obtained by two downscaling methods: a dynamical downscaling, where the IGSM is linked to a three-dimensional atmospheric model; and a statistical downscaling, where a pattern scaling algorithm uses climate-change patterns from 17 climate models. This framework allows for key sources of uncertainty in future projections of regional climate change to be accounted for: emissions projections; climate system parameters (climate sensitivity, strength of aerosol forcing and ocean heat uptake rate); natural variability; and structural uncertainty. Results show that the choice of climate policy and the climate parameters are the largest drivers of uncertainty. We also find that different initial conditions lead to differences in patterns of change as large as when using different climate models. Finally, this analysis reveals the wide range of possible climate change over Northern Eurasia, emphasizing the need to consider all sources of uncertainty when modeling climate impacts over Northern Eurasia.

Contents

1. INTRODUCTION

Northern Eurasia accounts for 60% of the land area north of 40°N and includes roughly 70% of the Eartt's boreal forest and more than two-thirds of the Earth's permafrost (Groisman *et al.*, 2009). As a result, the region is a major player in the global carbon budget. Over the past century, Northern Eurasia has experienced dramatic climate change, such as significant increases in temperature, growing season length, floods and droughts (Groisman and Soja, 2009; Soja and Groisman, 2012). These changes have large environmental and socioeconomic impacts including forest fires (Groisman *et al.*, 2007), permafrost thaw (Romanovsky *et al.*, 2007), extensive land-use change and water management projects (Groisman *et al.*, 2009). Further climate change could lead to significant releases of greenhouse gas (carbon dioxide and methane) to the atmosphere caused by severe permafrost thaw, increasing forest fires, changes in lake and wetland dynamics and changes in land cover. This implies a potential positive feedback cycle. For this reason, it is imperative to quantify the full range of possible climate change over Northern Eurasia.

[*] Joint Program on the Science and Policy of Global Change, Massachusetts Institute of Technology, Cambridge, MA.
[†] Corresponding author (Email: emonier@mit.edu).

Recent studies have investigated various climate change impacts over Northern Eurasia, including rising methane emissions (Zhu *et al.*, 2011), vegetation change (Tchebakova *et al.*, 2009; Jiang *et al.*, 2012), agroclimatic potential (Tchebakova *et al.*, 2011) and near-surface permafrost degradation (Lawrence and Slater, 2005). These studies, along with many others focused on Northern Eurasia or other regions, generally rely on a small ensemble of climate simulations that does not cover the full range of uncertainty. In particular, such studies do not consider all the major sources of uncertainty in future projections of climate change, namely: (i) uncertainty in the emissions projections, using different climate policies; (ii) uncertainty in the climate system parameters, represented by different values of climate parameters; (iii) natural variability, obtained by initial condition perturbation; and (iv) structural uncertainty using different climate models. For this reason they are likely to underestimate the range of climate change and its impacts over the region.

In this study, we attempt to simulate possible future climate change over Northern Eurasia, by computing probabilistic projections of 21st century surface air temperature and precipitation changes and considering the four aforementioned sources of uncertainty. Our focus is the Northern Eurasian Earth Science Partnership Initiative (NEESPI) domain, which extends from 15°E in the west to the Pacific Coast in the east from 40° to the Arctic Ocean coast in the north.

2. METHODOLOGY

2.1 Modeling Framework

This work uses the MIT IGSM (Sokolov *et al.*, 2005, 2009), an integrated assessment model that coupled an Earth System Model of Intermediate Complexity (EMIC), with a two-dimensional zonal-mean atmosphere, to a human activity model. The IGSM includes a representation of terrestrial water, energy, and ecosystem processes, global scale and urban chemistry including 33 chemical species, carbon and nitrogen cycle, thermodynamical sea ice, and ocean processes. The IGSM has been used in EMIC intercomparison exercises (Eby *et al.*, 2013; Zickfeld *et al.*, 2013) as well as to perform probabilistic projections based on uncertainties in emissions and climate parameters (Sokolov *et al.*, 2009; Webster *et al.*, 2012). In version 2.2, the IGSM uses a two-dimensional mixed layer anomaly diffusive ocean model. In version 2.3, the IGSM uses a three-dimensional dynamical ocean model based on the MIT ocean general circulation model Marshall *et al.* (1997a,b). In the IGSM2.3, heat and freshwater fluxes are anomaly coupled in order to simulate a realistic ocean state. Observed wind stress from six-hourly National Centers for Environmental Prediction (NCEP) reanalysis (Kalnay *et al.*, 1996) is used to more realistically capture surface wind forcing over the ocean. For any given model calendar year, a random calendar year of wind stress data is applied to the ocean in order to ensure that both short-term and interannual variability are represented in the ocean's surface forcing. Different random sampling can be applied to simulate different natural variability (Monier *et al.*, 2013b).

Regional climate change is then obtained from IGSM simulations using two downscaling methods. A dynamical downscaling method relies on the MIT IGSM-CAM framework (Monier *et al.*, 2013b) that links the IGSM version 2.3 to the National Center for Atmospheric Research

(NCAR) Community Atmosphere Model (CAM) (Collins *et al.*, 2006). New modules were developed and implemented in CAM to allow climate parameters to be changed to match those of the IGSM. In particular, the climate sensitivity of CAM is changed using a cloud radiative adjustment method (Sokolov and Monier, 2012). In the IGSM-CAM framework, CAM is driven by greenhouse gas concentrations and aerosol loading computed by the IGSM model, as well as by IGSM sea surface temperature (SST) anomalies. A statistical downscaling is based on a Taylor-expansion pattern scaling algorithm (Schlosser *et al.*, 2012) that extends the latitudinal projections of the IGSM two-dimensional zonal-mean atmosphere by applying longitudinally resolved climate patterns from observations and from climate model projections from the Coupled Model Intercomparison Project phase 3 (CMIP3). This two-pronged approach simulates regional climate change at 2° x 2.5° resolution based on IGSM probabilistic projections. It has been used successfully in previous work on the United States (Monier *et al.*, 2013a).

2.2 Description of the Simulations

In this study, we analyze two emissions scenarios corresponding to a median unconstrained emissions (UCE) scenario where no policy is implemented after 2012 and a stabilization scenario where greenhouse gases are stabilized at 550 ppm CO_2 (660 ppm CO_2-equivalent) by 2100. The stabilization scenario corresponds to the level 2 stabilization (L2S) described in Clarke *et al.* (2007).

For each emissions scenario, a 400-member ensemble simulation with the IGSM2.2 is run with Latin hypercube sampling (LHS) of climate parameters (climate sensitivity, strength of the aerosol forcing, ocean heat uptake rate) (Sokolov *et al.*, 2009; Webster *et al.*, 2012). Pattern scaling is then applied to each IGSM2.2 ensemble member based on the patterns of climate change of 17 CMIP3 climate models, following Schlosser *et al.* (2012). The resulting meta-ensemble is viewed as a “hybrid frequency distribution” (HFD) that integrates the uncertainty in the IGSM ensemble and in the regional patterns of climate change of different climate models.

Additional simulations are conducted with the IGSM-CAM framework in order to complement the statistical downscaling with simulations using a three-dimensional atmospheric model. To limit the number of IGSM-CAM simulations, three sets of climate parameters are chosen to reproduce the median, and the 5^{th} and 95^{th} percentiles of the probability distribution of 21^{st} century global climate change (Monier *et al.*, 2013b). The ocean heat uptake rate in all the IGSM-CAM simulations lies between the mode and the median of the probability distribution obtained with the MIT IGSM using optimal fingerprint diagnostics in Forest *et al.* (2008). We then choose values of climate sensitivity (CS) and net aerosol forcing (F_{ae}) that correspond to the 5^{th} percentile (CS=2.0°C and F_{ae}=-0.25 W/m^2), the median (CS=2.5°C and F_{ae}=-0.55 W/m^2) and the 95^{th} percentile (CS=4.5°C and F_{ae}=-0.85 W/m^2) of the marginal posterior probability density function with uniform prior for the climate sensitivity-net aerosol forcing (CS-F_{ae}) parameter space (Monier *et al.*, 2013b). The values of climate sensitivity agree well with the conclusions of the Fourth Assessment Report (AR4) of the Intergovernmental Panel on Climate Change (IPCC), which finds that the climate sensitivity is likely to lie in the range of 2.0°C to 4.5°C (Meehl *et al.*, 2007). Finally, five-member ensembles were carried out for each choice of parameters using different initial conditions and random wind sampling (referred to as initial conditions in the remainder of the paper). Further details on the IGSM-CAM simulations can be found in Monier *et al.* (2013b).

In total, this study is based on 13,600 IGSM-HFD simulations and 30 IGSM-CAM simulations, providing an unprecedented ensemble of simulations using both dynamical and statistical downscaling. From here on, we refer to low, median and high IGSM-HFD simulations, the IGSM-HFD simulations corresponding to the 5th, median and 95th percentile of the NEESPI mean distribution of temperature or precipitation. Similarly, we refer to low, median and high IGSM-CAM simulations, the IGSM-CAM simulations with values of climate sensitivity corresponding to the 5th, median and 95th percentile of its probability distribution, respectively, 2.0°C, 2.5°C and 4.5°C.

3. RESULTS

Figure 1 shows 21st century time series of NEESPI mean surface air temperature and precipitation anomalies from present day from IGSM-CAM and IGSM-HFD simulations. Even though the low, median and high simulations for each downscaling method are obtained from different distributions (NEESPI mean for IGSM-HFD and climate sensitivity for IGSM-CAM), the NEESPI mean simulated by the two methods show a good agreement, especially for temperature. For precipitation, the IGSM-CAM tends to simulate stronger increases in precipitation than the IGSM-HFD simulations, most notably for the stabilization scenario. That is because the IGSM-HFD takes into account multiple models, some with lesser tendencies for increases in precipitation over Northern Eurasia than CAM. Overall, both downscaling methods show a large range of future warming (from 4.5 to 10.0°C and from 2.0 to 4.0°C for, respectively, the unconstrained and the stabilization scenario) and moistening (from 0.2 to 0.5 mm/day and from 0.05 to 0.25 mm/day for, respectively, the unconstrained and the stabilization scenario) over the NEESPI region. The stabilization scenario is always associated with a significant reduction in future climate change compared to the unconstrained emissions scenario. It should be noted that all of the IGSM-HFD simulations exhibits warming and moistening for both emissions scenarios, indicating the robustness of these tendencies amongst the CMIP3 climate models over the region. In addition, the IGSM-CAM simulations exhibit a much larger year-to-year variability than the IGSM-HFD, even in the mean of the 5-member ensemble based on different initial conditions. That is because the variability in the IGSM-HFD is solely driven by the IGSM two-dimensional atmosphere, thus underestimating local variability over the NEESPI region. The envelope of the 30 IGSM-CAM simulations, which takes into account year-to-year variability, shows a good agreement with the observed variability in NEESPI mean temperature and precipitation anomalies from 2000 to 2010. Finally, Figure 1 reveals that the natural variability simulated by the IGSM-CAM provides a wider range of changes than the human signal simulated in IGSM-HFD until around 2040 when it is overcome by anthropogenically driven warming/moistening.

Another analysis comparing NEESPI mean changes in temperature and precipitation between the IGSM-CAM and IGSM-HFD is presented in **Figure 2**. We compare IGSM-HFD frequency distributions of NEESPI mean temperature and precipitation changes for various periods of the 21st century with respect to present day to the range obtained from the IGSM-CAM simulations. Figure 2 further demonstrates the broad agreement between the two downscaling methods and the large range of plausible future warming and moistening over Northern Eurasia. A further analysis (not shown) reveals that the frequency distributions generally display a positive skewness and kurtosis (relative to the normal distribution). The positive skewness and kurtosis increase as the projections extend into the 21st century, and are larger for the unconstrained emissions scenario. The IGSM-CAM simulations also exhibit positive skewness, although it is more pronounced than for the IGSM-HFD. This can be explained by the fact that the IGSM-CAM simulations only

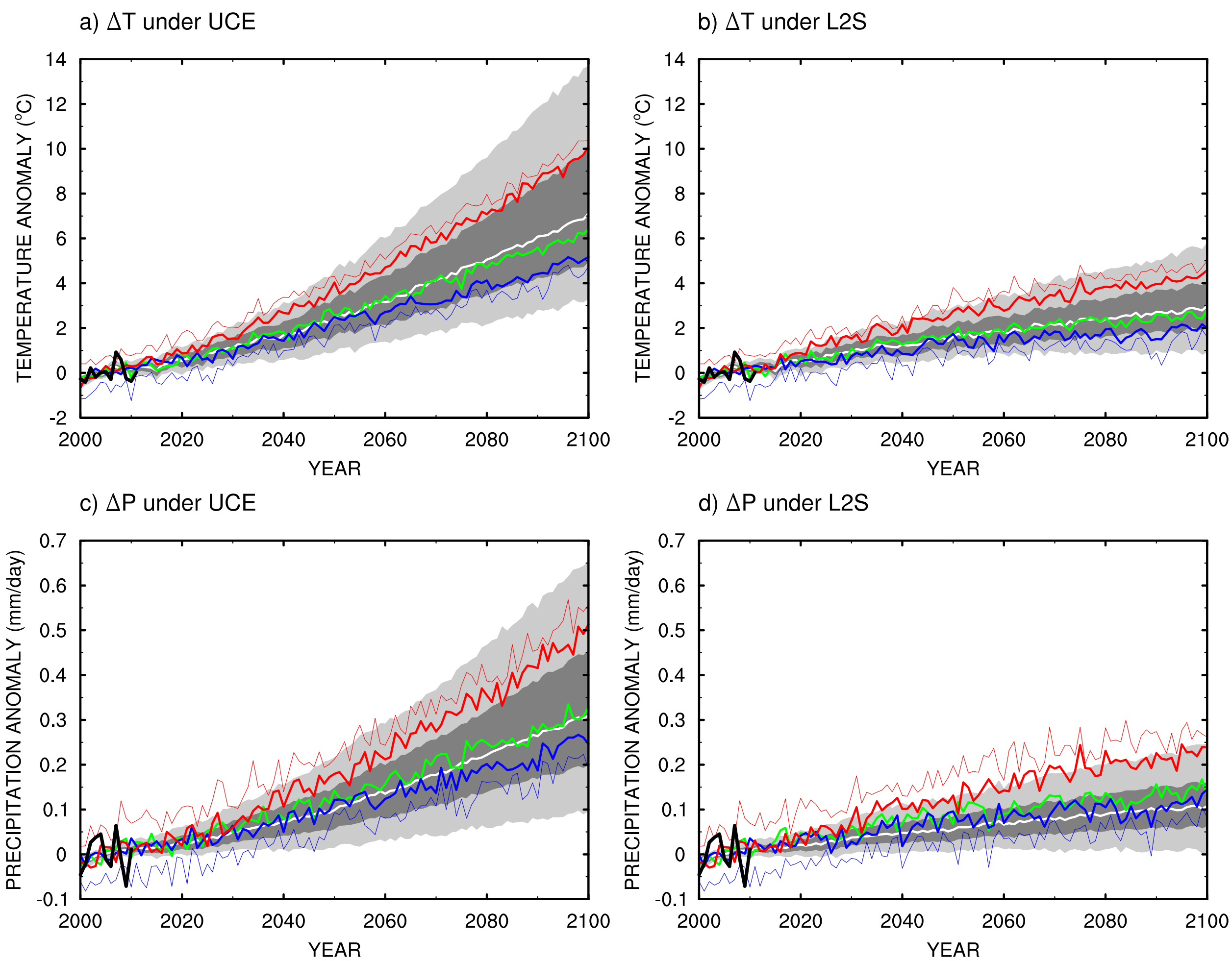

Figure 1. IGSM-CAM and IGSM-HFD changes in NEESPI mean surface air temperature under a) UCE scenario and b) L2S scenario; and in NEESPI mean total precipitation under c) UCE scenario and d) L2S scenario from the 1991–2010 base period. Light gray (dark gray) denotes the full range (90% probability interval) of the IGSM-HFD simulations while the white line shows the median. Bold blue, green and red lines show the 5-member ensemble mean of the IGSM-CAM simulations for the low, median and high values of climate sensitivity chosen in this study, while the thin blue and red lines show the minimum and maximum changes over all IGSM-CAM simulations. The black lines represent observations, the Goddard Institute for Space Studies (GISS) surface temperature (GISTEMP) (Hansen *et al.*, 2010) and the 20th Century Reanalysis V2 precipitation (Compo *et al.*, 2011).

consider one value of ocean heat uptake rate and that the marginal posterior probability density function with uniform prior for the climate sensitivity-net aerosol forcing (CS-F_{ae}) parameter space for this particular value of ocean heat uptake rate is itself skewed (Monier *et al.*, 2013b). Figure 2 also illustrates the overestimation of precipitation increases from the IGSM-CAM compared to the IGSM-HFD. In addition, it shows that full range of the IGSM-CAM simulations in the earlier part of 21st century, largely driven by natural variability, can be as wide as the full range of the IGSM-HFD simulations. This suggests that the role of natural variability in driving the range of probable NEESPI regional changes is not negligible, especially for projections over the next few decades.

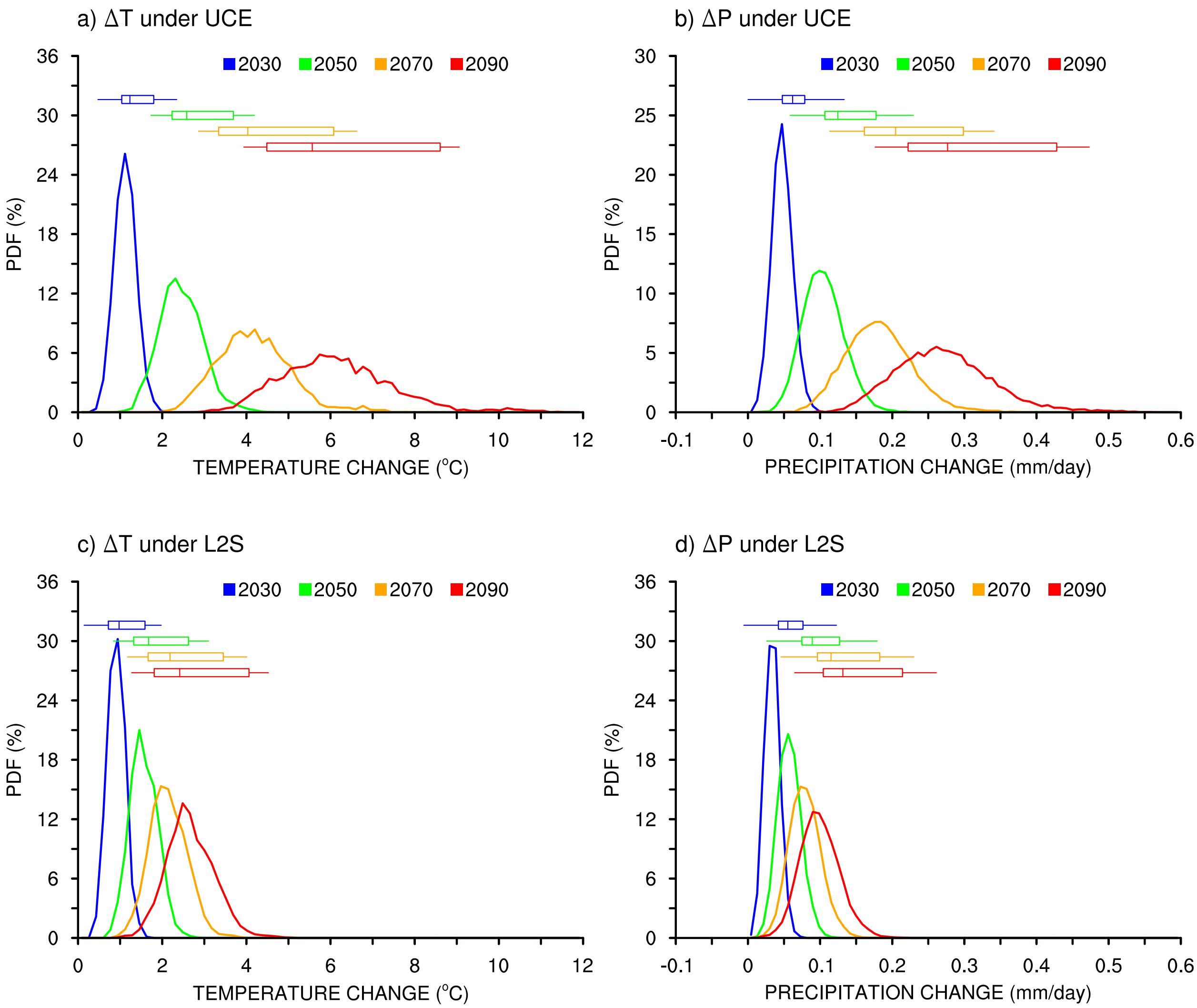

Figure 2. Hybrid frequency distributions (histograms) of changes in NEESPI mean surface air temperature and NEESPI mean total precipitation from the 1991–2010 base period along with the range obtained from the IGSM-CAM simulations (box plots). The box plots represent the changes obtained from the IGSM-CAM 5-member ensemble mean simulations with the low, median and high climate sensitivity while the horizontal line shows the minimum and maximum changes obtained among all individual IGSM-CAM simulations. Changes for different periods are shown with different colors: 2021–2040 mean (blue), 2041–2060 mean (green), 2061–2080 mean (orange) and 2081–2100 mean (red).

The regional patterns of change over the NEESPI region simulated by the IGSM-CAM and IGSM-HFD approaches are then investigated. **Figure 3** and **Figure 4** show maps of, respectively, 21st century changes in temperature and precipitation for the low, median and high simulations. Regional patterns of temperature changes agree well between the IGSM-CAM and IGSM-HFD, with the largest warming in the northern parts of the NEESPI region. For precipitation, there is also a broad agreement in the pattern of drying/moistening between the two downscaling approaches, with some drying in Eastern Europe and the southern parts of the NEESPI region and moistening in the northern parts. The IGSM-CAM simulations show similar patterns of temperature and precipitation changes, with larger magnitudes for higher climate sensitivities and emissions. This is because the IGSM-CAM relies on a single atmospheric model and because Figure 3 and Figure 4 show the average over the five initial conditions. Averaging over the different initial conditions filters out most of the natural variability, leaving only the human induced climate response, which displays similar patterns of change even with different values of climate sensitivity (Sokolov and Monier, 2012). On the other hand, the IGSM-HFD simulations show larger differences in the patterns of change because they consider multiple models and thus includes structural uncertainty.

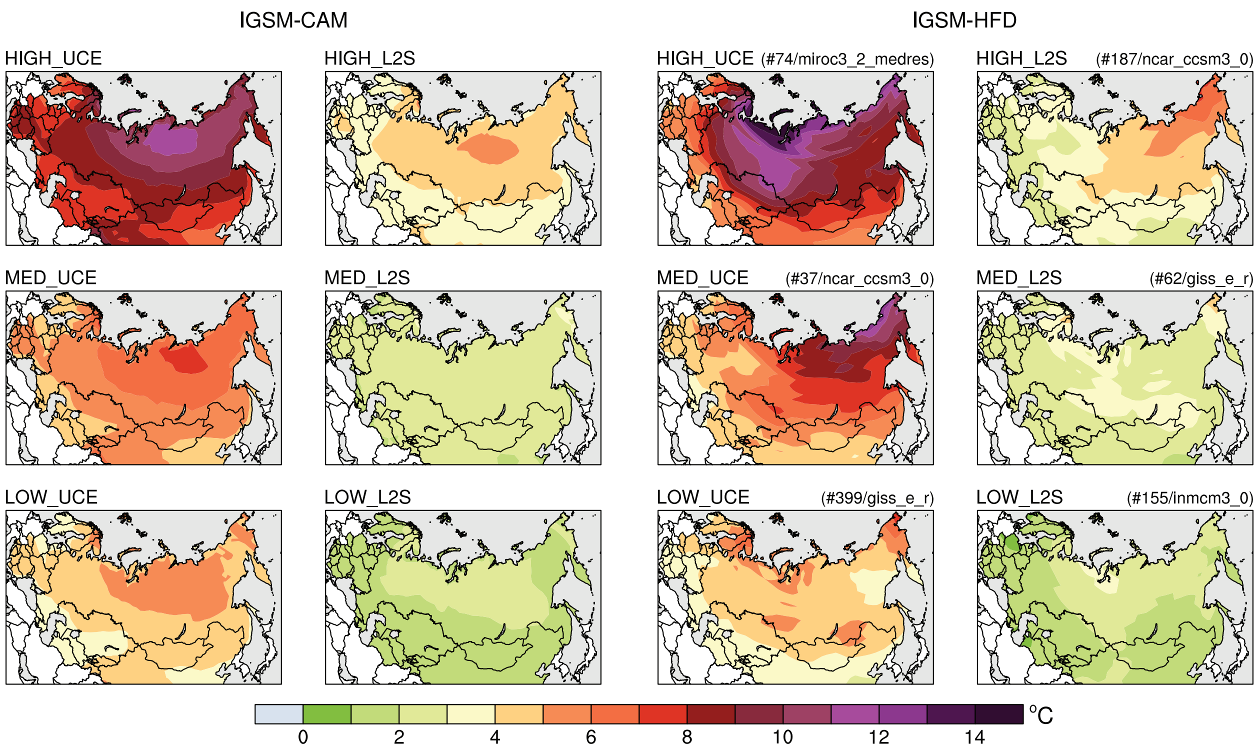

Figure 3. Maps of changes in surface air temperature for the period 2081–2100 relative to the 1991–2010 base period for both IGSM-CAM and IGSM-HFD simulations. For IGSM-CAM simulations, the 5-member ensemble mean for the high (HIGH), median (MED) and low (LOW) climate sensitivity are shown for the UCE and L2S scenarios. For the IGSM-HFD, the simulations corresponding to the 5th percentile (LOW), median (MED) and 95th percentile (HIGH) of the hybrid frequency distribution of NEESPI mean changes are shown for the UCE and L2S scenarios. The IGSM run number and model pattern are listed for the IGSM-HFD simulations plotted.

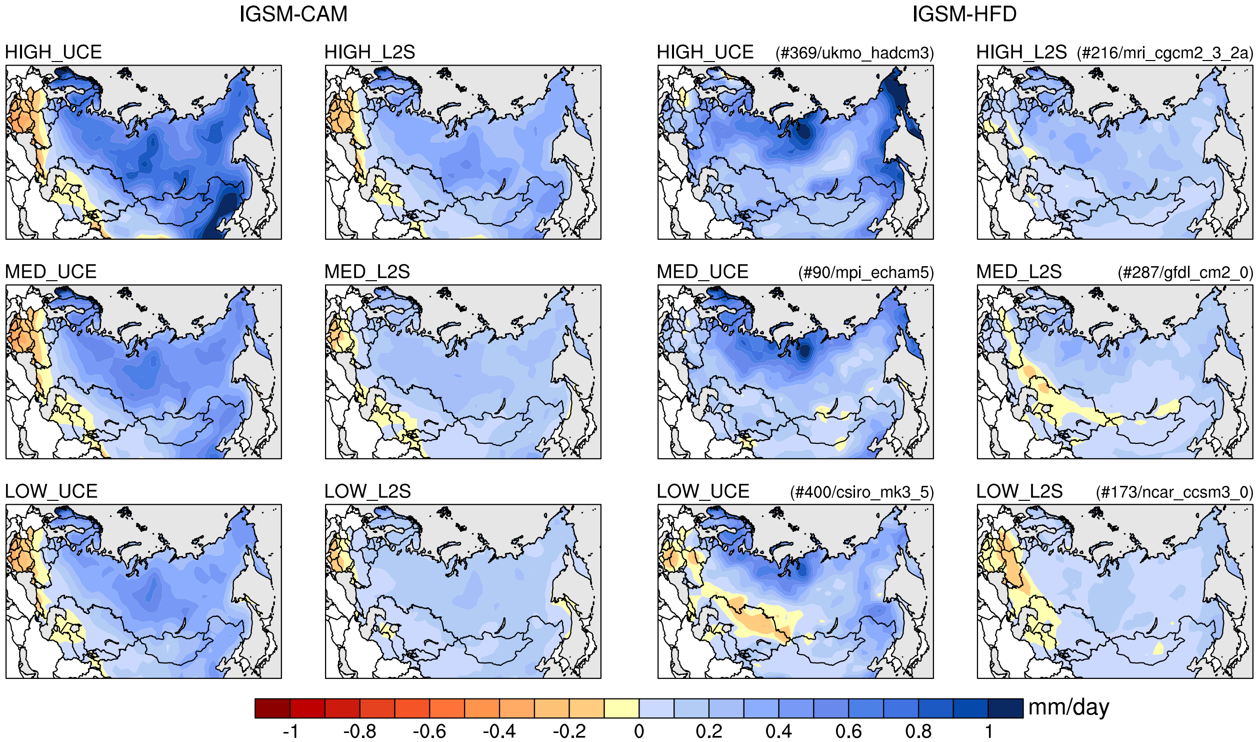

Figure 4. Maps of changes in total precipitation for the period 2081–2100 relative to the 1991–2010 base period for both IGSM-CAM and IGSM-HFD simulations. For IGSM-CAM simulations, the 5-member ensemble mean for the high (HIGH), median (MED) and low (LOW) climate sensitivity are shown for the UCE and L2S scenarios. For the IGSM-HFD, the simulations corresponding to the 5th percentile (LOW), median (MED) and 95th percentile (HIGH) of the hybrid frequency distribution of NEESPI mean changes are shown for the UCE and L2S scenarios. The IGSM run number and model pattern are listed for the IGSM-HFD simulations plotted.

Figure 5 shows the impact of the initial conditions within the IGSM-CAM framework. Maps of 21st century changes in temperature and precipitation for the median simulation under the stabilization scenario and for different initial conditions reveal the significant role of natural variability in future climate projections over Northern Eurasia. With different initial conditions, the simulations show similar magnitudes in temperature and precipitation changes but very different patterns. The location of the maximum warming can differ significantly, from European Russia (initial condition 3) to Eastern Siberia (initial condition 5). Precipitation patterns are also strongly influenced by the initial conditions, with a significantly different extent of the drying pattern found over Eastern Europe and the southern parts of the NEESPI region. The location of the maximum moistening can vary widely, from Scandinavia (initial condition 4) to Northern China (initial condition 2). The impact of the model pattern in the IGSM-HFD approach is analyzed by plotting the median simulation under the stabilization scenario and the four surrounding simulations, corresponding to the 50.02th, 50.01th, 49.99th and 49.98th percentiles of the NEESPI mean distribution (**Figure 6**). The NEESPI mean of these five simulations is virtually identical and each simulation could be considered as the median. However, the associated pattern of change is often very different because the corresponding model used in the pattern scaling

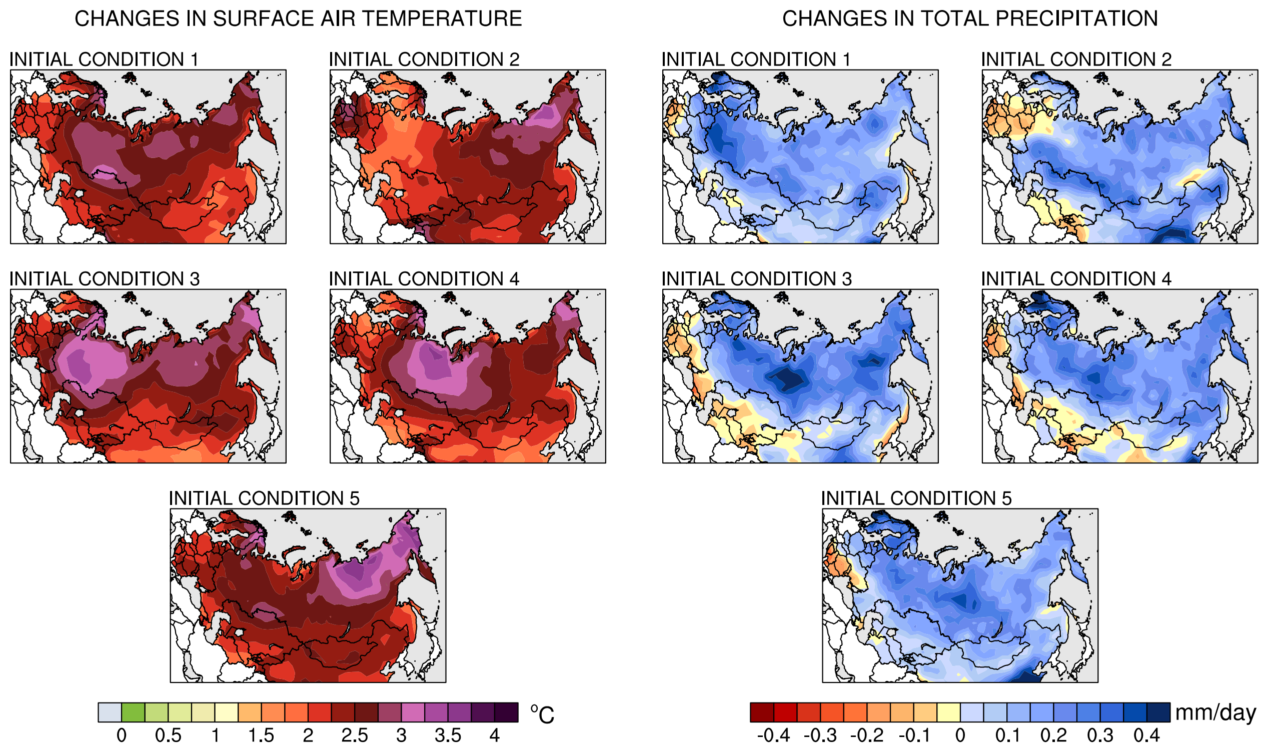

Figure 5. Maps of IGSM-CAM changes in surface air temperature and total precipitation for the period 2081–2100 relative to the 1991–2010 base period for the 5 simulations with different initial conditions for the median (MED) climate sensitivity and L2S scenario.

method is different. This leads to differences in temperature patterns similar to the initial condition analysis, with different locations of the maximum warming. For precipitation changes, the five IGSM-HFD simulations show less discrepancies than the initial condition analysis, largely because three out of the five simulations rely on the same model, and because the other two are based on models that seem to have similar patterns of precipitation changes over Northern Eurasia. This is a surprising result that shows that the uncertainty in regional climate change simulated by ensembles based on initial condition perturbation and multimodel ensembles seems to compare well over Northern Eurasia.

4. SUMMARY AND CONCLUSION

In this study, we present probabilistic projections of climate change over Northern Eurasia (NEESPI region) using the MIT IGSM downscaled via both a dynamical method (the IGSM-CAM framework) and a statistical method (pattern scaling). The analysis of the very large ensemble of simulations (a total of of 13,630 simulations) shows that the uncertainty in the choice of policy and in the climate response (climate sensitivity, strength of the aerosol forcing and ocean heat uptake rate) results in a wide range of probable outcomes. It further shows that simulations with different initial conditions can lead to different patterns of change (even in the 20-year mean changes), as different as using different models. This is especially true for lower values of climate sensitivity and emissions scenarios with stringent stabilization of greenhouse

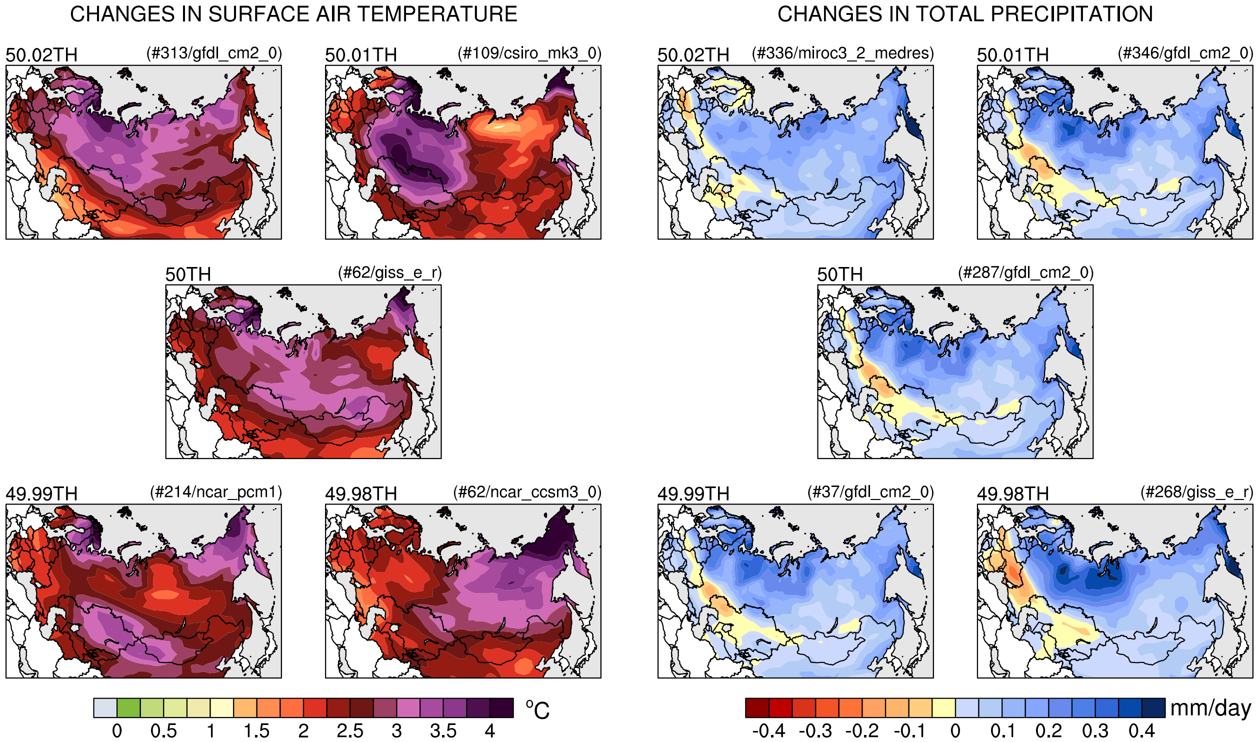

Figure 6. Maps of IGSM-HFD changes in surface air temperature and total precipitation for the period 2081–2100 relative to the 1991–2010 base period corresponding to the median (50TH) of the hybrid frequency distribution of NEESPI mean changes, along with the 4 simulations bounding the median (50.02TH, 50.01TH, 49.99TH and 49.98TH). The IGSM run number and model pattern are listed for the IGSM-HFD simulations plotted.

gases. This result agrees with Deser *et al.* (2012) that shows that natural variability contributes substantially to the uncertainty in climate change projections. This result suggests that an ensemble based on initial condition perturbation could potentially be used within a single model as a substitute for a multimodel ensemble, even for end-of-century projections. However, this study, along with Monier *et al.* (2013a), suggests that at the scale of a region like Northern Eurasia or the United States, the choice of policy is the largest source of uncertainty, followed by the climate parameters. This is especially true for long-term projections that extend past 2050.

In light of these projections, it appears obvious that Northern Eurasia is at risk of substantial climate warming if mitigation policies are not implemented. In light of recent observed trends, such warming could lead to further widespread permafrost degradation and more intense and frequent forest fires (Groisman *et al.*, 2007), and potentially result in the release of large amounts of carbon and methane (Gao *et al.*, 2013). The simulations with different emissions scenarios, values of climate parameters, initial conditions and models show consistent patterns of drying in the southern parts of the NEESPI region, especially over Eastern Europe, and moistening over the rest of the region. These pronounced features indicate potential predictability in future precipitation changes over the region.

Overall, we recommend that when investigating climate change impacts over Northern Eurasia, studies consider the four sources of uncertainty analyzed in this paper, namely: (i) uncertainty in the emissions projections, using different climate policies; (ii) uncertainty in the climate system parameters, represented by different values of climate parameters; (iii) natural variability, using different initial conditions; and (iv) structural uncertainty using different climate models. Furthermore, we suggest that probabilistic projections be used to drive impact models, even though we realize it would require large computing capabilities and would put a larger burden on impact modeling groups. Nonetheless, in light of this study, it appears evident that uncertainty in regional climate change projections is still large and should be accounted for systematically when estimating regional climate impacts.

Acknowledgements

We would like to recognize the Northern Eurasian Earth Science Partnership Initiative (NEESPI) for providing the background that made this study possible. This work was partially funded by the U.S. Department of Energy, Office of Biological and Environmental Research, under grant DE-FG02-94ER61937. The Joint Program on the Science and Policy of Global Change is funded by a number of federal agencies and a consortium of 40 industrial and foundation sponsors. (For the complete list see http://globalchange.mit.edu/sponsors/current.html). This research used the Evergreen computing cluster at the Pacific Northwest National Laboratory. Evergreen is supported by the Office of Science of the US Department of Energy under Contract No. DE-AC05-76RL01830. 20th Century Reanalysis V2 data provided by the NOAA/OAR/ESRL PSD, Boulder, Colorado, USA, from their Web site at http://www.esrl.noaa.gov/psd/.

5. REFERENCES

Clarke, L. E., J. A. Edmonds, H. D. Jacoby, H. M. Pitcher, J. M. Reilly and R. G. Richels, 2007: CCSP synthesis and assessment product 2.1, Part A: scenarios of greenhouse gas emissions and atmospheric concentrations. U.S. Climate Change Science Program, Department of Energy, Washington, DC 154 p.

Collins, W., C. Bitz, M. Blackmon, G. Bonan, C. Bretherton, J. Carton, P. Chang, S. Doney, J. Hack, T. Henderson *et al.*, 2006: The community climate system model version 3 (CCSM3). *J. Climate*, **19**(11): 2122–2143. doi:10.1175/JCLI3761.1.

Compo, G., J. Whitaker, P. Sardeshmukh, N. Matsui, R. Allan, X. Yin, B. Gleason, R. Vose, G. Rutledge, P. Bessemoulin *et al.*, 2011: The Twentieth Century Reanalysis Project. *Quart. J. Roy. Meteor. Soc.*, **137**(654): 1–28. doi:10.1002/qj.776.

Deser, C., A. Phillips, V. Bourdette and H. Teng, 2012: Uncertainty in climate change projections: the role of internal variability. *Clim. Dyn.*, **38**(3-4): 527–546. doi:10.1007/s00382-010-0977-x.

Eby, M., A. Weaver, K. Alexander, K. Zickfeld, A. Abe-Ouchi, A. Cimatoribus, E. Crespin, S. Drijfhout, N. Edwards, A. Eliseev, G. Feulner, T. Fichefet, C. Forest, H. Goosse, P. Holden, F. Joos, M. Kawamiya, D. Kicklighter, H. Kienert, K. Matsumoto, I. Mokhov, E. Monier, S. Olsen, J. Pedersen, M. Perrette, G. Philippon-Berthier, A. Ridgwell, A. Schlosser, T. Schneider von Deimling, G. Shaffer, R. Smith, R. Spahni, A. Sokolov, M. Steinacher, K. Tachiiri, K. Tokos, M. Yoshimori, N. Zeng and F. Zhao, 2013: Historical and idealized climate model experiments: an intercomparison of Earth system models of intermediate complexity. *Clim. Past*, **9**: 1111–1140. doi:10.5194/cp-9-1111-2013.

Forest, C. E., P. H. Stone and A. P. Sokolov, 2008: Constraining climate model parameters from observed 20th century changes. *Tellus*, **60A**(5): 911–920. doi:10.1111/j.1600-0870.2008.00346.x.

Gao, X., C. A. Schlosser, A. P. Sokolov, K. W. Anthony, Q. Zhuang and D. Kicklighter, 2013: Permafrost degredation, methane and their biogeochemical climate-warming feedback. *Environ. Res. Lett.*

Groisman, P., E. A. Clark, V. M. Kattsov, D. P. Lettenmaier, I. N. Sokolik, V. B. Aizen, O. Cartus, J. Chen, S. Conard, J. Katzenberger, O. Krankina, J. Kukkonen, T. Machida, S. Maksyutov, D. OJima, J. Qi, V. E. Romanovsky, M. Santoro, C. C. Schmullius, A. I. Shiklomanov, K. Shimoyama, H. H. Shugart, J. K. Shuman, M. A. Sofiev, A. I. Sukhinin, C. Vörösmarty, D. Walker and E. F. Wood, 2009: The Northern Eurasia Earth Science Partnership: An Example of Science Applied to Societal Needs. *Bull. Amer. Meteor. Soc.*, **90**: 671–688. doi:10.1175/2008BAMS2556.1.

Groisman, P. and A. J. Soja, 2009: Ongoing climatic change in Northern Eurasia: justification for expedient research. *Environ. Res. Lett.*, **4**(045002). doi:10.1088/1748-9326/4/4/045002.

Groisman, P. Y., B. G. Sherstyukov, V. N. Razuvaev, R. W. Knight, J. G. Enloe, N. S. Stroumentova, P. H. Whitfield, E. Forland, I. Hannsen-Bauer, H. Tuomenvirta, H. Aleksandersson, A. V. Mescherskaya and T. R. Karl, 2007: Potential forest fire danger over Northern Eurasia: Changes during the 20th century. *Global Planet. Change*, **56**: 371–386. doi:10.1016/j.gloplacha.2006.07.029.

Hansen, J., R. Ruedy, M. Sato and K. Lo, 2010: Global surface temperature change. *Rev. Geophys.*, **48**(4): RG4004. doi:10.1029/2010RG000345.

Jiang, Y., Q. Zhuang, S. Schaphoff, S. Sitch, A. Sokolov, D. Kicklighter and J. Melillo, 2012: Uncertainty analysis of vegetation distribution in the northern high latitudes during the 21st century with a dynamic vegetation model. *Ecology and Evolution*. doi:10.1002/ece3.85.

Kalnay, E., M. Kanamitsu, R. Kistler, W. Collins, D. Deaven, L. Gandin, M. Iredell, S. Saha, G. White, J. Woollen, Y. Zhu, M. Chelliah, W. Ebisuzaki, W. Higgins, J. Janowiak, K. C. Mo, C. Ropelewski, J. Wang, A. Leetmaa, R. Reynolds, R. Jenne and D. Joseph, 1996: The NCEP/NCAR 40-year reanalysis project. *Bull. Amer. Meteor. Soc.*, **77**(3): 437–471. doi:10.1175/1520-0477(1996)077<0437:TNYRP>2.0.CO;2.

Lawrence, D. and A. Slater, 2005: A projection of severe near-surface permafrost degradation during the 21st century. *Geophys. Res. Lett.*, **32**(24): L24401. doi:10.1029/2005GL025080.

Marshall, J., A. Adcroft, C. Hill, L. Perelman and C. Heisey, 1997a: A finite-volume, incompressible Navier Stokes model for studies of the ocean on parallel computers. *J. Geophys. Res.*, **102**(C3): 5753–5766. doi:10.1029/96JC02775.

Marshall, J., C. Hill, L. Perelman and A. Adcroft, 1997b: Hydrostatic, quasi-hydrostatic, and nonhydrostatic ocean modeling. *J. Geophys. Res.*, **102**(C3): 5733–5752. doi:10.1029/96JC02776.

Meehl, G., T. Stocker, W. Collins, P. Friedlingstein, A. Gaye, J. Gregory, A. Kitoh, R. Knutti, J. Murphy, A. Noda, S. Raper, I. Watterson, A. Weaver and Z.-C. Zhao, 2007: Global Climate Projections. In: *Climate Change 2007: The Physical Science Basis. Contribution of Working Group I to the Fourth Assessment Report of the Intergovernmental Panel on Climate Change*,

S. Solomon, D. Qin, M. Manning, Z. Chen, M. Marquis, K. B. Averyt, M. Tignor and H. L. Miller, (eds.), Cambridge University Press, Cambridge, United Kingdom and New York, NY, USA., Chapter 8, pp. 747–845.

Monier, E., X. Gao, J. Scott, A. Sokolov and C. A. Schlosser, 2013a: A framework for modeling uncertainty in regional climate change. *Climatic Change*, **in revisions**.

Monier, E., J. Scott, A. Sokolov, C. Forest and C. Schlosser, 2013b: An integrated assessment modelling framework for uncertainty studies in global and regional climate change: the MIT IGSM-CAM (version 1.0). *Geosci. Model Dev. Discuss.*, **6**: 2213–2248. doi:10.5194/gmdd-6-2213-2013.

Romanovsky, V. E., T. S. Sazonova, V. T. Balobaev, N. I. Shender and D. O. Sergueev, 2007: Past and recent changes in air and permafrost temperatures in Eastern Siberia. *Global Planet. Change*, **56**: 399–413.

Schlosser, C. A., X. Gao, K. Strzepek, A. Sokolov, C. Forest, S. Awadalla and W. Farmer, 2012: Quantifying the Likelihood of Regional Climate Change: A Hybridized Approach. *J. Climate*. doi:10.1175/JCLI-D-11-00730.1.

Soja, A. J. and P. Y. Groisman, 2012: Northern Eurasia Earth Science Partnership Initiative: evolution of scientific investigations to applicable science. *Environ. Res. Lett.*, **7**(045201). doi:10.1088/1748-9326/7/4/045201.

Sokolov, A. and E. Monier, 2012: Changing the Climate Sensitivity of an Atmospheric General Circulation Model through Cloud Radiative Adjustment. *J. Climate*, **25**(19): 6567–6584. doi:10.1175/JCLI-D-11-00590.

Sokolov, A. P., C. A. Schlosser, S. Dutkiewicz, S. Paltsev, D. Kicklighter, H. D. Jacoby, R. G. Prinn, C. E. Forest, J. M. Reilly, C. Wang, B. Felzer, M. C. Sarofim, J. Scott, P. H. Stone, J. M. Melillo and J. Cohen, 2005: The MIT Integrated Global System Model (IGSM) Version 2: Model Description and Baseline Evaluation. MIT Joint Program on the Science and Policy of Global Change *Report 124*, July, 40 p. (http://globalchange.mit.edu/files/document/MITJPSPGC_Rpt124.pdf).

Sokolov, A. P., P. H. Stone, C. E. Forest, R. Prinn, M. C. Sarofim, M. Webster, S. Paltsev, C. A. Schlosser, D. Kicklighter, S. Dutkiewicz, J. Reilly, C. Wang, B. Felzer, J. M. Melillo and H. D. Jacoby, 2009: Probabilistic Forecast for Twenty-First-Century Climate Based on Uncertainties in Emissions (Without Policy) and Climate Parameters. *J. Climate*, **22**(19): 5175–5204. doi:10.1175/2009JCLI2863.1.

Tchebakova, N. M., E. Parfenova and A. J. Soja, 2009: The effects of climate, permafrost and fire on vegetation change in Siberia in a changing climate. *Environ. Res. Lett.*, **4**(045013). doi:10.1088/1748-9326/4/4/045013.

Tchebakova, N. M., E. I. Parfenova, G. I. Lysanova and A. J. Soja, 2011: Agroclimatic potential across central Siberia in an altered twenty-first century. *Environ. Res. Lett.*, **6**(045207). doi:10.1088/1748-9326/6/4/045207.

Webster, M., A. P. Sokolov, J. M. Reilly, C. E. Forest, S. Paltsev, C. A. Schlosser, C. Wang, D. Kicklighter, M. Sarofim, J. Melillo, R. G. Prinn and H. D. Jacoby, 2012: Analysis of Climate Policy Targets under Uncertainty. *Climatic Change*, **112**(3-4): 569–583. doi:10.1007/s10584-011-0260-0.

Zhu, X., Q. Zhuang, M. Chen, A. Sirin, J. Melillo, D. Kicklighter, A. Sokolov and L. Song, 2011: Rising methane emissions in response to climate change in Northern Eurasia during the 21st century. *Environ. Res. Lett.*, **6**(045211). doi:10.1088/1748-9326/6/4/045211.

Zickfeld, K., M. Eby, A. Weaver, E. Crespin, T. Fichefet, H. Goose, G. Philippon-Berthier, N. Edwards, P. Holden, A. Eliseev, I. Mokhov, G. Feulner, H. Kienert, M. Perrette, T. Schneider von Deimling, C. Forest, F. Joos, R. Spahni, M. Steinacher, M. Kawamiya, K. Tachiiri, D. Kicklighter, E. Monier, A. Schlosser, A. Sokolov, K. Matsumoto, K. Tokos, S. Olsen, J. Pedersen, G. Shaffer, A. Ridgewell, N. Zeng and F. Zaho, 2013: Long-term Climate Change Commitment and Reversibility: An EMIC Intercomparison. *J. Climate*. doi:10.1175/JCLI-D-12-00584.1.

FOR THE COMPLETE LIST OF JOINT PROGRAM REPORTS:
http://globalchange.mit.edu/pubs/all-reports.php

200. A Strategy for a Global Observing System for Verification of National Greenhouse Gas Emissions *Prinn et al.* June 2011

201. Russia's Natural Gas Export Potential up to 2050 *Paltsev* July 2011

202. Distributional Impacts of Carbon Pricing: *A General Equilibrium Approach with Micro-Data for Households* *Rausch et al.* July 2011

203. Global Aerosol Health Impacts: *Quantifying Uncertainties* *Selin et al.* August 201

204. Implementation of a Cloud Radiative Adjustment Method to Change the Climate Sensitivity of CAM3 *Sokolov and Monier* September 2011

205. Quantifying the Likelihood of Regional Climate Change: *A Hybridized Approach* *Schlosser et al.* October 2011

206. Process Modeling of Global Soil Nitrous Oxide Emissions *Saikawa et al.* October 2011

207. The Influence of Shale Gas on U.S. Energy and Environmental Policy *Jacoby et al.* November 2011

208. Influence of Air Quality Model Resolution on Uncertainty Associated with Health Impacts *Thompson and Selin* December 2011

209. Characterization of Wind Power Resource in the United States and its Intermittency *Gunturu and Schlosser* December 2011

210. Potential Direct and Indirect Effects of Global Cellulosic Biofuel Production on Greenhouse Gas Fluxes from Future Land-use Change *Kicklighter et al.* March 2012

211. Emissions Pricing to Stabilize Global Climate *Bosetti et al.* March 2012

212. Effects of Nitrogen Limitation on Hydrological Processes in CLM4-CN *Lee & Felzer* March 2012

213. City-Size Distribution as a Function of Socio-economic Conditions: *An Eclectic Approach to Down-scaling Global Population* *Nam & Reilly* March 2012

214. CliCrop: a Crop Water-Stress and Irrigation Demand Model for an Integrated Global Assessment Modeling Approach *Fant et al.* April 2012

215. The Role of China in Mitigating Climate Change *Paltsev et al.* April 2012

216. Applying Engineering and Fleet Detail to Represent Passenger Vehicle Transport in a Computable General Equilibrium Model *Karplus et al.* April 2012

217. Combining a New Vehicle Fuel Economy Standard with a Cap-and-Trade Policy: *Energy and Economic Impact in the United States* *Karplus et al.* April 2012

218. Permafrost, Lakes, and Climate-Warming Methane Feedback: *What is the Worst We Can Expect?* Gao et al. May 2012

219. Valuing Climate Impacts in Integrated Assessment Models: *The MIT IGSM* *Reilly et al.* May 2012

220. Leakage from Sub-national Climate Initiatives: *The Case of California* *Caron et al.* May 2012

221. Green Growth and the Efficient Use of Natural Resources *Reilly* June 2012

222. Modeling Water Withdrawal and Consumption for Electricity Generation in the United States *Strzepek et al.* June 2012

223. An Integrated Assessment Framework for Uncertainty Studies in Global and Regional Climate Change: *The MIT IGSM* *Monier et al.* June 2012

224. Cap-and-Trade Climate Policies with Price-Regulated Industries: *How Costly are Free Allowances?* *Lanz and Rausch* July 2012.

225. Distributional and Efficiency Impacts of Clean and Renewable Energy Standards for Electricity *Rausch and Mowers* July 2012.

226. The Economic, Energy, and GHG Emissions Impacts of Proposed 2017–2025 Vehicle Fuel Economy Standards in the United States *Karplus and Paltsev* July 2012

227. Impacts of Land-Use and Biofuels Policy on Climate: *Temperature and Localized Impacts* *Hallgren et al.* August 2012

228. Carbon Tax Revenue and the Budget Deficit: *A Win-Win-Win Solution?* *Sebastian Rausch and John Reilly* August 2012

229. CLM-AG: An Agriculture Module for the Community Land Model version 3.5 *Gueneau et al.* September 2012

230. Quantifying Regional Economic Impacts of CO2 Intensity Targets in China *Zhang et al.* September 2012

231. The Future Energy and GHG Emissions Impact of Alternative Personal Transportation Pathways in China *Kishimoto et al.* September 2012

232. Will Economic Restructuring in China Reduce Trade-Embodied CO_2 Emissions? *Qi et al.* October 2012

233. Climate Co-benefits of Tighter SO_2 and NO_x Regulations in China *Nam et al.* October 2012

234. Shale Gas Production: *Potential versus Actual GHG Emissions* *O'Sullivan and Paltsev* November 2012

235. Non-Nuclear, Low-Carbon, or Both? *The Case of Taiwan* *Chen* December 2012

236. Modeling Water Resource Systems under Climate Change: *IGSM-WRS* *Strzepek et al.* December 2012

237. Analyzing the Regional Impact of a Fossil Energy Cap in China *Zhang et al.* January 2013

238. Market Cost of Renewable Jet Fuel Adoption in the United States *Winchester et al.* January 2013

239. Analysis of U.S. Water Resources under Climate Change *Blanc et al.* February 2013

240. Protection of Coastal Infrastructure under Rising Flood Risk *Lickley et al.* March 2013

241. Consumption-Based Adjustment of China's Emissions-Intensity Targets: *An Analysis of its Potential Economic Effects* *Springmann et al.* March 2013

242. The Energy and CO_2 Emissions Impact of Renewable Energy Development in China *Zhang* et al. April 2013

243. Integrated Economic and Climate Projections for Impact Assessment *Paltsev et al.* May 2013

244. A Framework for Modeling Uncertainty in Regional Climate Change *Monier et al* May 2013

245. Climate Change Impacts on Extreme Events in the United States: An Uncertainty Analysis *Monier and Gao* May 2013

246. Probabilistic Projections of 21st Century Climate Change over Northern Eurasia *Monier et al.* July 2013